



# Modified Kirchhoff prestack depth migration using the Gaussian beam operator as Green function – Theoretical and numerical results

Carlos A. S. Ferreira, João C. R. Cruz

Center of Geosciences, CPGf, Federal University of Pará, Brazil

Copyright 2005, SBGf – Sociedade Brasileira de Geofísica

This paper was prepared for presentation at the 9<sup>th</sup> International Congress of the Brazilian Geophysical Society held in Salvador, Brazil, 11-14 September 2005.

Contents of this paper were reviewed by the Technical Committee of the 9<sup>th</sup> International Congress of the Brazilian Geophysical Society. Ideas and concepts of the text are authors' responsibility and do not necessarily represent any position of the SBGf, its officers or members. Electronic reproduction or storage of any part of this paper for commercial purposes without the written consent of the Brazilian Geophysical Society is prohibited.

## Abstract

The Gaussian Beam concept has been of great importance for works on modeling, migration and inversion, during the last two decades. This work then joins the flexibility of the true amplitude (diffraction stack) Kirchhoff migration process with the regularity of the high frequency Gaussian Beam description of the wavefield as Green function, in some simple numerical examples of geophysical exploration interest. Our process can be named as Kirchhoff-Gaussian Beam Prestack Depth Migration (KGB-PSDM) in a true amplitude sense.

## Introduction

During the I and II workshops of research on explorational risks for oil and gas, on the behalf of the Cooperative Research Network (CRN) (UFPA, UFBA, UFRN, UFAL, UFC and UFPE), held successively in Natal-RN and Belém-PA, Brazil, last year, we have presented the theoretical and numerical results of a true-amplitude, prestack, Kirchhoff-type depth migration process (Ferreira and Cruz, 2004 a,b) using the concept of Gaussian Beams (Popov, 1996; Červený, 2000; Červený, 2001) as Green function of the imaging problem. In summary, the migration operator considered in this case is the same as treated in Schleicher et al. (1993), but presently it is modified so that the analytical particle displacement is represented by a superposition of Gaussian Beams (GBs).

By using the main characteristics of the GBs superposition integral, such as its description in any point inside the considered medium (e.g., over structural interfaces or over the Earth surface) and the Fresnel volume elements (Hubral et al., 1993; Schleicher et al., 1997), we have projected the integration domain of the GBs superposition integral, in some point somewhere inside the medium, over a given surface (fictitious or not), towards the projected Fresnel zone of the seismic experiment, over the (Earth) acquisition surface. This procedure permitted to us to physically interpret the analytical expression of the GBs superposition weight-function (Klimeš, 1984) and keep unchanged another weight-function, the latter related to the true-amplitude migration process described in Schleicher et al. (1993). The insertion of the final GBs operator in terms of the

projected region (i.e., the Fresnel zone and the projected Fresnel zone) into the kernel of the Kirchhoff migration integral permits to interpret the diffraction stack process in two steps. For each point belonging to the diffraction surface, constructed for each source-receiver pair and for each point to be imaged in depth, its projected Fresnel zone on the Earth surface is determined. In the following, we stack the traces in the data domain that are restricted to a beam inside the predetermined Fresnel zone and input the result referred to the reference trace into its Huygens surface. Next, the diffraction stack is performed along this surface and the result is placed into its depth position.

In this work we show the main numerical results obtained so far using the modified Kirchhoff operator cited above. We include as examples the imaging of structures that range from plane reflectors (dipping or not) to curved reflectors, all derived from classical examples found by exploration seismic. Although the velocity model considered a priori is simple, we show that the migration process is able to preserve amplitude and that can be used in several other types of analyses, such as AVO/AVA and multiple diffraction stack (Tygel et al., 1993).

## Method

The migration operator to be considered, in the frequency domain, is (Schleicher et al., 1993)

$$\hat{V}(M, \omega) = -\frac{i\omega}{2\pi} \int_A d\xi_1 d\xi_2 w(M, \vec{\xi}) U(\vec{\xi}, \omega) e^{i\omega\tau_D(M, \vec{\xi})} \quad (1)$$

where  $A$  is the migration aperture,  $M = M(x, z)$  is an arbitrary point in depth,  $w(M, \vec{\xi})$  is the weight-function that corrects the seismic amplitudes from its geometrical spreading losses,  $\vec{\xi} = (\xi_1, \xi_2)^T$  is a coordinate vector that parameterizes the positions of sources and geophones along the acquisition surface,  $\tau_D(M, \vec{\xi})$  is the Huygens (diffraction) surface and  $U(\vec{\xi}, \omega)$  is the analytical particle displacement, formed by the real particle displacement  $u(\vec{\xi}, \omega)$  plus its Hilbert transform, as imaginary part. The superscript  $T$  means transposition.

In the present work, we consider that the analytical particle displacement  $U(\vec{\xi}, \omega)$  is represented by the following expression

$$U(\vec{\xi}, \omega) = \int_{A_p} d\xi_1^p d\xi_2^p \frac{\det \Lambda}{\det \mathbf{H}_F} \frac{\det \mathbf{Q}(\vec{\xi}^p)}{\cos \theta_G} \Phi(\vec{\xi}^p) \times A(\vec{\xi}^p) e^{-i\omega \tau_R(\vec{\xi}, \vec{\xi}^p)}, \quad (2)$$

where  $\mathbf{H}_F$  is the Fresnel zone matrix (Schleicher et al., 2004),  $\Lambda = \Gamma_S^T \mathbf{N}_{SR} + \Gamma_G^T \mathbf{N}_{GR}^T$ , where  $\mathbf{N}_{SR}$  and  $\mathbf{N}_{GR}$  are second time traveltimes derivatives matrices, according to Schleicher et al. (1993), while  $\Gamma_S^T$  and  $\Gamma_G^T$  are matrices related to the data acquisition geometry. All those matrices are  $2 \times 2$ . The coordinate vector  $\vec{\xi}^p = (\xi_1^p, \xi_2^p)^T$  belongs to a subset of the migration aperture  $A$ , corresponding to the projected Fresnel zone, here denominated by  $A_p$ . In this work, we consider that only the *first* Fresnel zone defines  $A_p$ .  $\det \mathbf{Q}(\vec{\xi}^p)$  and  $\cos \theta_G$  are the geometrical spreading and the emergence angle at  $G$  (geophone), respectively. Eq. (2) is a complex conjugate form of the modeling integral used to construct synthetic seismograms using the Gaussian Beam concept. The weight-function  $\Phi(\vec{\xi}^p)$  is a quantity that asymptotically reduces Eq. (2) to the zero order ray theory solution (Červený, 2000). In this work, it is represented by (Ferreira and Cruz, 2004 a,b)

$$\Phi(\vec{\xi}^p) = \frac{i\omega}{2\pi} \sqrt{\det \mathbf{H}_F} (\det \mathbf{Q}(\vec{\xi}^p))^{-1} \cos \theta_G. \quad (3)$$

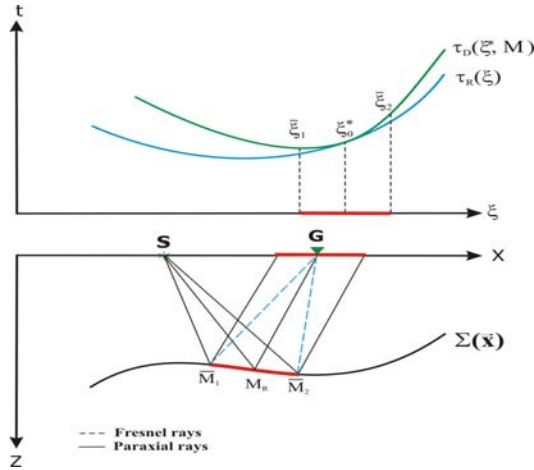


**Figure 1** – 2D sketch of a seismic experiment showing the specular ray  $SM_R G$ , its Fresnel zone in depth, the corresponding paraxial rays and the projected Fresnel zone. Point  $\vec{\xi}_0^*$  is a stationary point belonging to the Huygens curve. The paraxial point  $\vec{\xi}_1$  and  $\vec{\xi}_2$  belong to the same reflection curve.

This weight-function was established under the assumption that it is proportional to the difference between the wavefront curvatures of two types of waves,

one representing the central ray and the other representing the paraxial rays nearby. Intuitively, this lead us to the idea that this difference could be proportional to the Fresnel zone of the experiment. It is a well known fact that when a seismic ray reflects over a given surface, at some reflection point  $M_R$ , the wavefield is “smeared” around this point, precisely in Fresnel zones around the reflection point. In our interpretation, then, Eq. (3) simply states the fact that the paraxial rays that influence the wavefield observed at some reflection point  $M_j$  are those points belonging to a *certain* Fresnel zone (preferably the first) in depth. In other words, we stress the strong constraint imposed by Eq. (3): in the numerical implementation, only those rays located inside the (first) Fresnel zone shall be considered by Eq. (2). At the same time, this asymptotically reduces the same equation to the zero order ray theory solution.

Finally,  $A(\vec{\xi}^p) e^{-i\omega \tau_R(\vec{\xi}, \vec{\xi}^p)}$  represents the paraxial contribution in the positions  $\vec{\xi}^p$  that influences the observations in  $\vec{\xi}$ , where  $\tau_R(\vec{\xi}, \vec{\xi}^p)$  is the complex traveltimes in  $\vec{\xi}$  due to a observation in  $\vec{\xi}^p$ .

Inserting Eq. (2) in (1), making use of Eq. (3), the final migration operator in the time domain is given by

$$V(M, t) = \frac{1}{4\pi^2} \int_A d\xi_1 d\xi_2 w(\vec{\xi}, M) \int_{A_p} d\xi_1^p d\xi_2^p \sqrt{\det \mathbf{H}_p} \times \ddot{U}[\vec{\xi}, t + \tau_D(\vec{\xi}, \vec{\xi}^p, M)]. \quad (4)$$

Here  $\mathbf{H}_p = \Lambda^T \mathbf{H}_F^{-1} \Lambda$  is the projected Fresnel zone matrix (Schleicher et al., 2004), while the double dots indicate second derivatives with respect to time of the analytical particle displacement.

In Figure 1 we present a geometrical explanation of Eq. (4). In 2D, we depict the representation of a seismic experiment in which a specular ray  $SM_R G$  and its paraxial Fresnel rays  $SM_j G$  ( $j = 1, 2, \dots, n$ ) determine a set of points over a given reflector, known as Fresnel zone (Schleicher et al., 2004), as well as its projection towards the seismic acquisition surface. According to the diffraction stack theory (Schleicher et al., 1993), point  $\vec{\xi}_0^*$  is a stationary point corresponding to the reflection event in  $M_R$  and that belongs to the Huygens surface exactly at the tangency point, where the reflection and diffraction curves coincide. With the determination of the projected first Fresnel zone, we look for points  $\vec{\xi}_j$  belonging to this (first) zone, and that are part of the same reflection curve, corresponding to the neighbor point of  $M_R$  in depth.

### Synthetic examples

We have implemented Eq. (4) for the imaging of geological structures containing plane and curved reflectors, immersed in an homogeneous media where the layers present constant velocities. We consider that the models are formed by a single one reflector in depth, above them the  $P$ -waves velocities are  $v_1 = 2000$  Km/s

and below them the velocities are  $v_2 = 3500$  Km/s. In order to generate synthetic data for the migration process, a 2.5D Kirchhoff modeling scheme was implemented, with a common-offset configuration using  $2h = 25$  m, in the first case, and  $2h = 15$  m, in the second case. In the case of the plane reflectors, the spacing among sources and geophones was 25m, while in the case of the curved reflector this spacing was set to 15m. The seismic wavelet used in the modeling experiment was zero phase Gabor wavelet, with dominant frequencies of 10 Hz and 20 Hz, with a total duration of 10ms and 20 ms, respectively. In the migration process, the inner GBs integral in Eq. (4) is a 2.5D of Eq. (2), where intra-plane factors were introduced in order to correctly simulate the amplitudes. It must be bear in mind that the introduction of this intra-plane factors does not affect the weight-function  $\Phi(\vec{\xi}^p)$  in the 2D case.

In all cases studied bellow, the Fresnel volume elements (in depth and projected towards the acquisition surface) were completed determined by using dynamic raytracing (DRT) (Červený, 2001). The initial conditions for the DRT system, then, are complex, which also allows the calculation of quantities that are used in the construction of the GBs (e.g., beam half-width, imaginary part of the geometrical spreading matrix). In order to guarantee beams with very narrow half-widths at the endpoints of the rays, we use the plane-wave condition at the geophones, using the criteria described in Müller (1984). Since the main objective of this work is the migration process, their respective synthetic data will not be shown. Only the image results will be considered.

- **Plane reflectors**

In this first example, we consider two plane reflectors, one horizontal, located at depth  $z = 2$  Km, and a second reflector dipping  $7^\circ$  to the left. In these examples we have used the following values for the discretization steps in the  $x$  and  $z$  directions:  $\Delta x = \Delta z = 25$ m.

In Figure 2a we have the result of the conventional Kirchhoff migration for the case of the horizontal reflector. Since the velocity model is assumed to be the true one, the migration process correctly reconstructed the reflector in its depth position. Also, as it is known, border artifacts are generated due to insufficient data to stack at those places (Hertweck et al., 2003). The KGB-PSDM migration, which considers the stacking of only those traces belonging to the projected Fresnel zone (Figure 2b), automatically eliminates these artifacts. Moreover, the image is less aliased with respect to the one obtained by the Kirchhoff process.

In the case of the dipping reflector (Figure 2c and 2d), the image is again reconstructed in its true depth position. In the Kirchhoff process, the same border effects are observed. In the KGB-PSDM process, on both borders the artefacts are not seen, except at some isolated places in the image, such as near the depths 200-400 m. But again the image obtained by the KGB-PSDM process is less aliased than the one obtained by the Kirchhoff process.

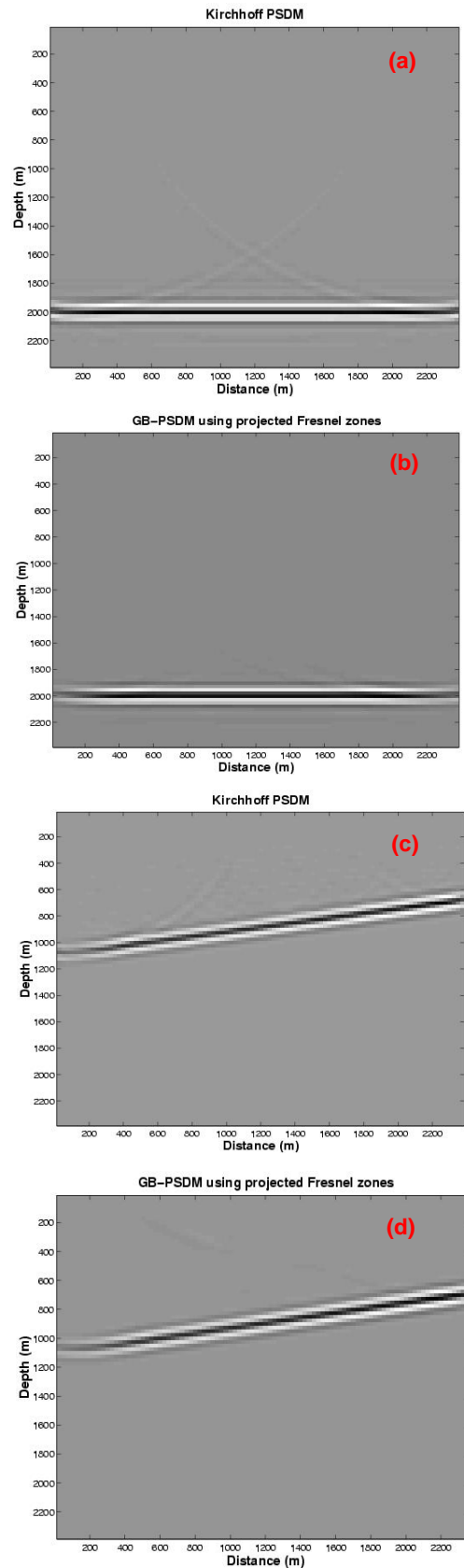
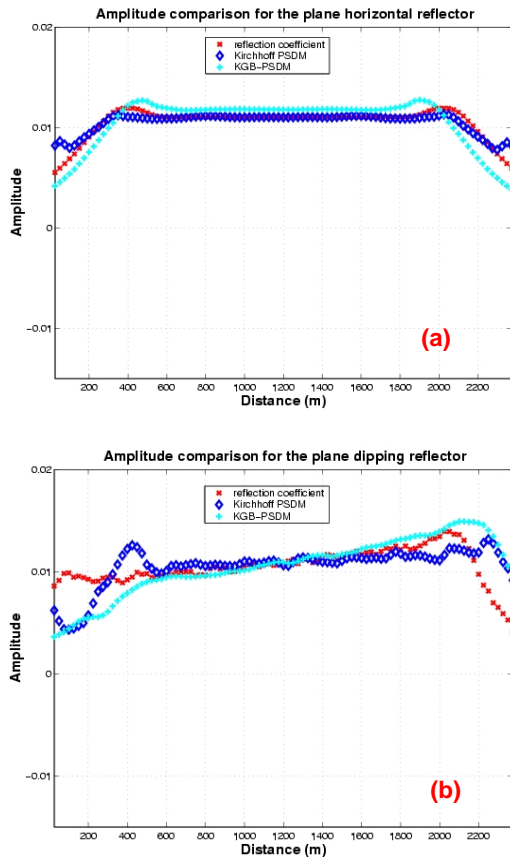


Figure 2 – Plane reflectors.

As for the amplitudes, in both cases there seems to exist suitable differences based on each case considered. In the horizontal plane reflector, the amplitudes behave well along the whole reflector, but near the borders, the image resolution seems to be reduced. This fact may be related to the stacking of an odd number of traces inside the Fresnel zone at the borders. However, as shown in Hertweck et al. (2003), the amplitude reconstruction in these position are only half of its true value, due to insufficient data to stack there. On the other hand, when we consider the dipping reflector case, this fact does not seem to influence in the final image. Either on the right border or on the left border, the amplitudes reconstructed by the KGB-PSDM process seem to be similar to the ones reconstructed by the Kirchhoff process.



**Figure 3** – Picked peak amplitudes for the plane reflectors. (a) Horizontal reflectors. (b) Dipping reflector.

In Figures 3a and 3b we make a comparison among the picked peak amplitudes obtained by the two true amplitude migration processes, taken along the two reflectors, and we have compared them to the amplitudes obtained by the modeling scheme. In the horizontal plane reflector case, we observe an excellent agreement in the trends of both curves, considering that along the whole reflector these amplitudes are overestimated by 3% of the original values. This is again related to the stacking of

more information for each point in depth, due to the influence in the amplitudes of its neighbour reflection points. On the other hand, on the borders occurs an underestimation of amplitudes, as previously commented and expected. However, the agreement in the behaviour of the amplitudes is considered excellent. For the dipping reflector case, where the situation seemed visually better at first sight, there occurs an overestimation on the left border, followed by an agreement in the trends upwards, ending in underestimation of amplitudes on the right border. Again, the agreement in the amplitude trends is considered excellent.

- **Curved reflectors**

In this particular case, we consider the existence of a curved reflector in the form of a syncline, located at a depth  $z = 0.8$  Km, where its trough reaches a depth of  $z = 1.1$  Km. In this case, the discretization steps in the  $x$  and  $z$  directions were:  $\Delta x = \Delta z = 15$  m.

In Figure 4a we have the result of the Kirchhoff migration process for the syncline case. Again borders effects inherent to the process are observed on the borders. In Figure 4b, we depict the result of the imaging using the KGB-PSDM process. We visually note a decrease of the border effects and a higher resolution in the final image.

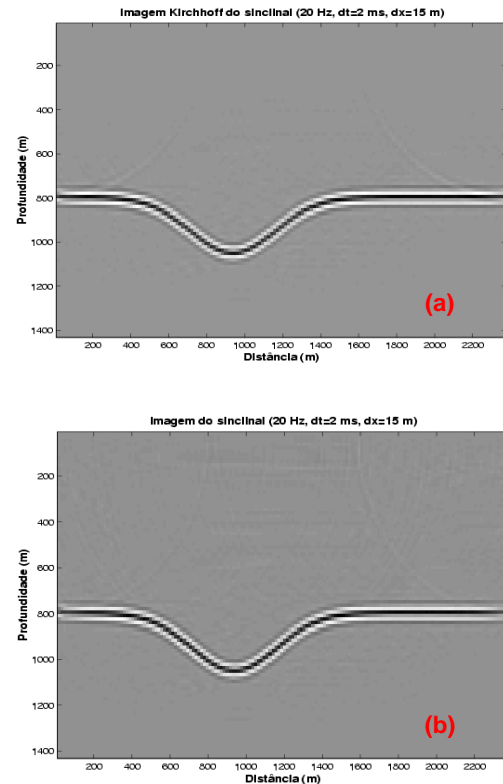


**Figure 4** – Curved reflectors.

For qualitative effects, Figure 5 shows the comparison of the two picked peak amplitudes along the reflector, considered by the two migration methods. We have not compared the amplitude picking of the two methods with

respect to the Kirchhoff 2.5D modeling scheme, due to the fact that the syncline model presents more than one single arrival in some geophones that record the arrival of the trough area, i.e. the caustic area. In fact, there exist up to three arrivals from this region, so that each observation should be isolated from the others (Tygel et al., 1998) in order to compare each of them with the ones obtained from the migration processes. Thus, we have chosen to compare only the amplitude pickings obtained by the two migration methods, where the ability of our algorithm in leading with caustics and multiple arrivals was tested in regions where the focusing of the wavefield generally occurs. We observe then that there occurs an excellent agreement in the trends of the amplitude curves, with some isolated particularities. In general, along the whole reflector the KGB-PSDM process shows itself equivalent to the Kirchhoff process. On the left of the curve we observe a small overestimation in the amplitudes, but with an excellent agreement in their trends. On the rest of the reflector, the behaviour of the amplitude curve for the KGB-PSDM process is in excellent agreement with the values of the amplitudes obtained by the Kirchhoff process, where again on the right border there occurs an underestimation in the values of the amplitudes. However, again all the amplitude trends are in excellent agreement when compared to the conventional process.

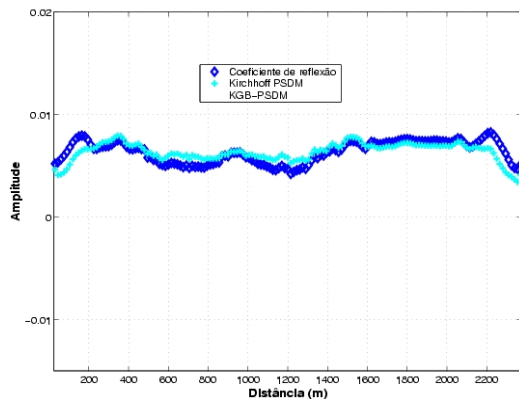


**Figure 5** – Amplitude comparison for the syncline model.

### Frequency content of the data

We shall discuss an important point that derives from the fact that Fresnel zones (FZs) are frequency dependent quantities. In modeling, the determination of FZs depends on their positions, on the acquisition geometry of the data and of the (dominant) frequency content of the seismic source (Schleicher et al., 1997; Schleicher et al., 2004). Although these are, to some extent, known and controlled quantities, they lead to the formation of FZs of different sizes along the pathway of a ray or over a given reflector surface. In the case of the reflector surface, the FZs shall also depend on the curvature of the reflector, since some sub-matrices of the Bornfeld's propagator depends on the

curvature of the reflector, in the case of a reflection point, and are essential to the calculation of the analytical form of the FZ matrix. In this case, it is reasonable to suppose that several FZs, of different sizes, are formed for one single reflector and, being projected towards the acquisition surface, they must also be present in the seismic data. Thus this means that this frequency range must be a priori known before migration. We shall illustrate this effect for the case of the syncline model.

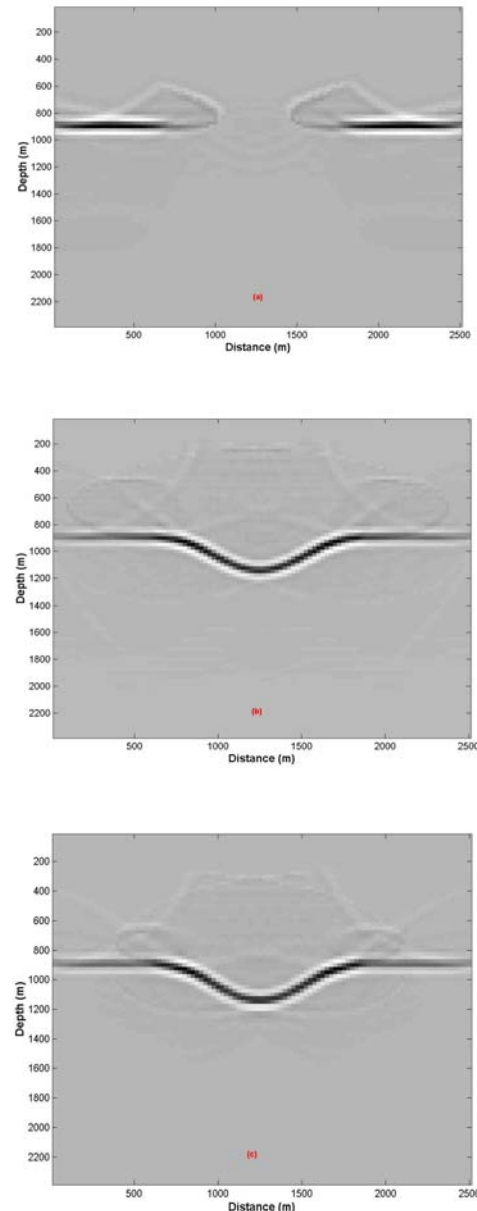


**Figure 6** – Frequency content of the data.

In Figure 6 we show three examples of imaging for the same geological model using different frequencies for the

FZs. In Figure 6a, we have the imaging using the dominant frequency (10 Hz) of the seismic signal. Only the flat parts of the syncline structures are correctly imaged. The trough of the syncline is not imaged, since the FZs there are not seen by the KGB-PSDM migration process. In Figures 6b and 6c we have used 50 Hz and 100 Hz, respectively. This time the trough is correctly imaged at the expense of the flat parts (borders). This indicates that, when imaging, the whole frequency spectrum must be considered. We propose then to rewrite Eq. (4) in the following form

$$V(M,t) = \frac{1}{4\pi^2} \int_A d\xi_1 d\xi_2 w(\vec{\xi}, M) \int_f df \int_{A_P} d\xi_1^P d\xi_2^P \sqrt{\det \mathbf{H}_P(\vec{\xi}^P, f)} \times \ddot{U}[\vec{\xi}, t + \tau_D(\vec{\xi}, \vec{\xi}^P, M)] \quad (5)$$

where in our interpretation  $\mathbf{H}_P = \mathbf{H}_P(\vec{\xi}^P, f)$  and the frequency content of each FZ is considered and is summed as a final input for the Kirchhoff summation.

### Conclusions

We have developed a true-amplitude prestack Kirchhoff-type depth migration process in which we considered as Green function an integral operator that represents a superposition of Gaussian beams.

We have tested the KGB-PSDM algorithm in the imaging of plane and curved geological models. In the plane models, we considered two distinct cases: an horizontal plane reflector and a dipping plane reflector. Both images were obtained considering a simple homogeneous velocity model. In both images, the KGB-PSDM considerably eliminated the presence of migration artifacts, yielding less aliased sections. Some visual lack of resolution eventually occurred, as in the case of the plane horizontal reflector, mainly due to the number of stacked traces inside each projected Fresnel zone on the borders. But, overall, both final images were less aliased than the ones obtained by the Kirchhoff process.

The comparison in the behaviour of amplitudes for these two cases showed several effects that are not visually seen in the images. In both cases, the tendency in amplitude trends are in excellent agreement, considering that on both borders sometimes occur overestimation and underestimation of amplitude values. Far from the borders, the KGB-PSDM process seems to overestimates the amplitude values in at least 3%. This fact is related to the stacking of informations referred to the neighbour reflection points in depth of the image point.

The KGB-PSDM algorithm has also been tested on curved reflectors, such as a syncline. While the image obtained by the Kirchhoff process showed the well known presence of migration artifacts, the KGB-PSDM process obtained a less aliased image. The comparison of amplitudes values recovered by both migration processes showed some similarities with the case of the plane reflectors, but also with an excellent agreement in the amplitude trends. In this particular example, we have only compared the amplitude values recovered by both migration processes, since in the syncline case there

occurs multiple arrivals from the caustic region located in the trough of the structure and this events should be first isolated for comparison reasons.

We have also tested the algorithm with the frequency content of the data. We have come to the conclusion that to reach a full imaging capacity, our operator must consider the whole spectrum of frequency present in the data. Due to this fact, we propose to rewrite the KGB-PSDM operator in order to consider the contribution of several FZs of different frequencies for each trace.

### Acknowledgments

The first author would like to thank the Brazilian National Research Council (CNPq-Brazil) for the financial support in the form of PhD scholarship, during all the stages of this research.

### References

- Červený, V., 2000. Summation of paraxial Gaussian beams and of paraxial ray approximations in inhomogeneous anisotropic layered structures. In: *Seismic Waves in Complex 3D Structures*, Report 10. Charles University, Prague, 121-159.
- Červený, V., 2001. *Seismic ray theory*. Oxford University Press.
- Ferreira, C. A. S.; Cruz, J. C. R., 2004a. Modified Kirchhoff prestack depth migration using the Gaussian Beam operator as Green function. In: *EAGE 66<sup>th</sup> Conference & Exhibition*. Paris, France. Expanded abstracts.
- Ferreira, C. A. S.; Cruz, J. C. R., 2004b. Migração pré-empilhamento em profundidade usando o operador de feixes gaussianos como função de Green – Teoria. I Workshop da Rede Cooperativa de Pesquisa em Risco Exploratório em Petróleo e Gás. Natal-RN, Brazil. Expanded abstracts.
- Hertweck, T.; Jäger, C.; Goertz, A.; Schleicher, J., 2003. Aperture effects in 2.5D Kirchhoff migration: a geometrical explanation. *Geophysics*, **68**, 1673-1684.
- Hubral, P.; Schleicher, J.; Tygel, M.; Hanitzsch, C., 1993. Determination of Fresnel zones from traveltimes measurements. *Geophysics*, **58**, 703-712.
- Müller, G., 1984. Efficient calculation of Gaussian Beams seismograms for two-dimensional inhomogeneous media. *Geophys. J. R. astr. Soc.*, **79**, 153-166.
- Popov, M. M., 1996. Ray theory and Gaussian beam method for geophysicists. PPPG, UFBA. 148p.
- Schleicher, J.; Tygel, M.; Hubral, P., 1993. 3D true-amplitude finite-offset migration. *Geophysics*, **58**, 1112-1126.
- Schleicher, J.; Hubral, P.; Tygel, M.; Jaya M. S., 1997. Minimum apertures and Fresnel zones in migration and demigration. *Geophysics*, **62**, 183-194.
- Schleicher, J.; Tygel, M.; Hubral, P., 2004. True-amplitude seismic imaging. *Soc. of Expl. Geophysicists*. (Submitted monography).
- Tygel, M.; Schleicher, J.; Hubral, P.; Hanitzsch, C., 1993. Multiple weights in diffraction stack migration. *Geophysics*, **58**, 1820-1830.
- Tygel, M.; Schleicher, J.; Hubral, P.; Santos, L. T., 1998. 2.5D true-amplitude Kirchhoff migration to zero-offset in laterally inhomogeneous media. *Geophysics*, **63**, 557-573.